HIGH SCHOOL EDITION
Journal of Student Research
Volume 13 Issue 3 (2024)

Nonlinear Dynamics of Magnetic Gears Using Two Fidget Spinners

Ethan Hyo Jeon[1] and Shawn Brooks[#]

[1]University of Toronto Schools, Canada
[#]Advisor

ABSTRACT

Magnetic gears, massive in scale or largely simplified, exhibit highly nonlinear and chaotic behaviour. We investigate the underlying phenomenon of rotation of fidget spinners with Neodymium (Nd) magnets placed at their ends through a theoretical and experimental lens. A simplified model is proposed, combining both the mechanics (i.e. nonlinear vibration of rotary mass-spring-damper system) and electromagnetics (i.e. Bio-Savart law and Larentz force) of such gears. We derive a governing equation using Newton's law and basic electromagnetic theories, solve it numerically via simulation, and explore rotation angle dissipation. Key parameters are then compared and matched across theory and experiment. This research has been motivated by one of the problems proposed for IYPT (International Young Physicists' Tournament) 2024.

Introduction

Magnetic gears present a new area of study combining the classical mechanics of gears (through their rotational motion) and magnetism (through the placement of equally spaced magnets on the gears). We see potential usage of magnetic gears in industrial settings for efficiently generating energy or reducing noise levels. Compared to mechanical gears, the benefits that magnetic gears provide cannot be overstated. They are more precise and reliable, as they can transmit motion to the other gear without coming into direct contact. Also, magnetic gears require significantly less lubrication and can utilize the strongest permanent magnets to generate substantially greater torque (Tlali et al., 2014).

In this paper, we will be investigating the fundamental behaviour of a simplified setup of a specific type of magnetic gears where two gears are placed on the same plane with axially magnetized disk magnets mounted along the circumference of the gears. Such form of magnetic gears can be realized by using two fidget spinners with Neodymium (Nd) magnets attached to their ends placed side by side on a plane so that each spinner gets attracted to the other one (Figure 1). When one of them is rotated, the other will start to rotate simply due to the interactions between magnetic fields. We will theoretically analyze and experimentally verify this motion, as well as observe the effect of varying key parameters.

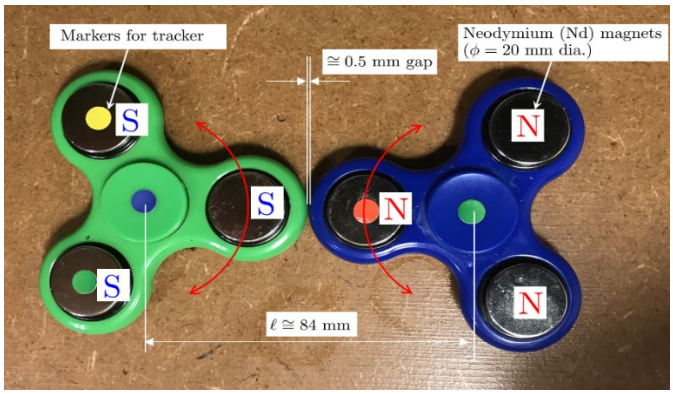

Figure 1. Two fidget spinners with Neodymium magnets attached at each end.

In order to understand the dynamics of fidget spinners in Figure 1, we need detailed analysis of the force between two permanent magnets. Recently, several studies have derived formulas to compute such forces. (Ravaud et al., 2010) using the equivalence between the Amperian current model and the Coulombian model of a magnet to show that a thin coil and an axially magnetized cylindrical magnet have the same mathematical model. Based on this, they derived an algebraic equation to compute the force between two cylindrical magnets. However, it is only applicable to situations where two cylindrical magnets are aligned co-axially. Similarly, (Vokoun et al., 2009) introduced an analytical expression for calculating the attraction force between two cylindrical permanent magnets whose axes are parallel but displaced by a certain distance. Yet their formula is not applicable to our situation in Figure 1 because placing two magnets on the same plane results in division by zero in their formula. Recently, there also has been an academic paper (Vila et al., 2019) which studied the mechanical vibration of a chain of magnetic gears using the fidget spinner as a magnetic gear unit. However, they arranged permanent magnets facing each other at the ends of fidget spinners, i.e. the cylindrical magnets are arranged coaxially when the gears are mated.

Based on our literature review, we observed the lack of an existing formula providing the magnetic force equation for two cylindrical (or disk) magnets placed on the same plane as Figure 1. This gave us the motivation to write this paper going through fundamental theories in electromagnetics (Biot-Savart law and Lorentz force theory) and developing our own analytical solutions to compute the required force.

Theory

Phenomenon

The nonlinear oscillation of the fidget spinner magnetic gear in Figure 1 can be explained using Figure 2 in a qualitative way. In a simplified version of the spinner motion where the right spinner is held at an initial deflection of just below $\pi/3$ radians, the magnetic fields nearly balance out (upper left figure in Figure 2). As soon as the right spinner is released, it begins to rotate counterclockwise. When it briefly passes the horizontal, it starts to pull the other magnet clockwise (upper right figure in Figure 2). Once both magnets come to a stop, the right magnet starts to turn in the other direction, again pulling the other magnet towards it (lower left figure in Figure 2). Once they coincide with the horizontal, the energy has now been shifted to the left magnet, and bi-directional energy transfer continues between both spinners (lower right figure in Figure 2).

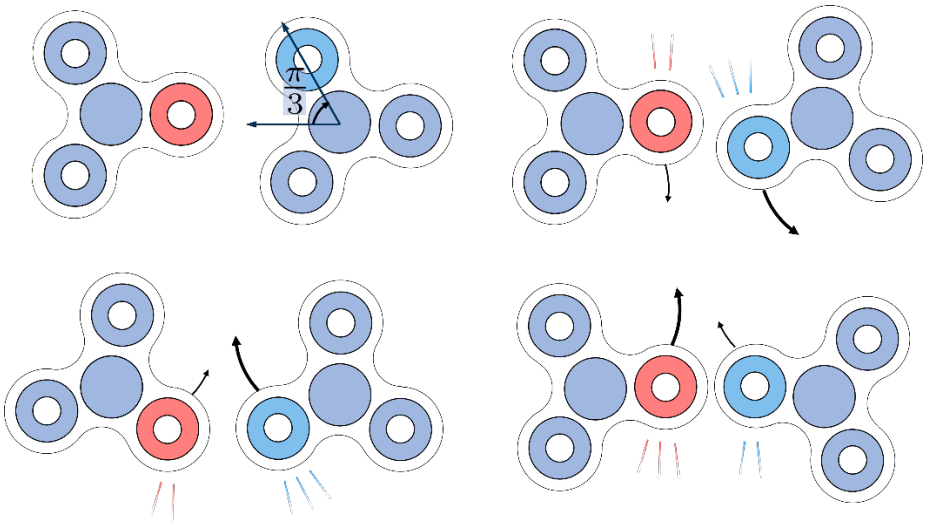

Figure 2. Qualitative behaviour of oscillation of the fidget spinner magnetic gears using snapshots. The sequence of the motion is as follows: upper left figure => upper right figure => lower left figure => lower right figure.

Mechanics

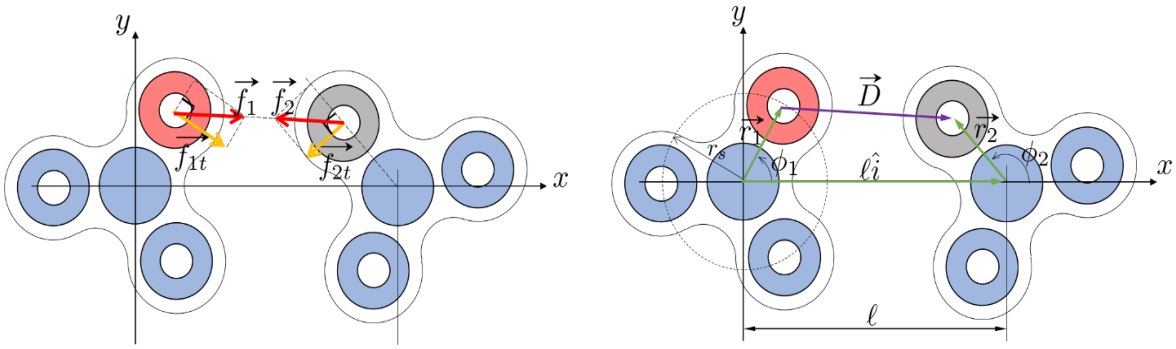

Figure 3. Forces applied to each fidget spinner created by Nd magnets. (Left figure) $\vec{f_1}$ is the force applied to the left spinner by the right spinner magnet, and $\vec{f_2}$ is the force applied to the right spinner by the left spinner magnet. The net force applied to each fidget spinner will be the tangential components of $\vec{f_1}$ and $\vec{f_2}$ which are denoted by $\vec{f_{1t}}$ and $\vec{f_{2t}}$ respectively for each spinner. (Right figure) Position vectors used to represent force vectors. $\hat{\imath}$ is the unit vector along x axis, $\vec{r_1}$ and $\vec{r_2}$ are position vectors of the center of each magnet in action. ϕ_1 and ϕ_2 are rotational angles of each fidget spinner. $\vec{D}$ is the position vector starting from the center of the left spinner to that of the right spinner.

The movement of each fidget spinner is created by the attractive magnetic force which can be represented by the force vectors $\vec{f_1}$ and $\vec{f_2}$ as shown in Figure 3. Two spinners will be in equilibrium when $\phi_1 = 0$ and $\phi_2 = \pi$. Note that the magnitude of these force vectors is the same (denoted by f_m), and their directions are opposite to each other along the same line of action (represented by the position vector $\vec{D}$). Therefore, we can express these magnetic force vectors using the unit vector along their direction as Equation 1.

Equation 1:

$$\overrightarrow{f_1} = f_m \frac{\vec{D}}{\|\vec{D}\|}, \overrightarrow{f_2} = -f_m \frac{\vec{D}}{\|\vec{D}\|}$$

The position vectors shown in the right side of Figure 3 can be written using the coordinate unit vectors as Equation 2:

Equation 2:

$$\begin{gathered}\overrightarrow{r_1} = r_s \cos\phi_1\, \hat{\imath} + r_s \sin\phi_1\, \hat{\jmath}, \\ \overrightarrow{r_2} = r_s \cos\phi_2\, \hat{\imath} + r_s \sin\phi_2\, \hat{\jmath}, \\ \vec{D} = -\overrightarrow{r_1} + \ell\hat{\imath} + \overrightarrow{r_2} = (-r_s \cos\phi_1 + \ell + r_s \cos\phi_2)\hat{\imath} - r_s(\sin\phi_1 - \sin\phi_2)\hat{\jmath}\end{gathered}$$

where ℓ is the distance between the centers of spinners, and r_s is the radius of the circle for the position of the magnet with respect to the center of the spinner, i.e. r_s is the magnitude of $\overrightarrow{r_1}$ and $\overrightarrow{r_2}$ vectors. (See the right figure of Figure 3 for more details of these parameters). Also, the magnitude of $\vec{D}$ is computed as follows in Equation 3:

Equation 3:

$$\|\vec{D}\| = \sqrt{\ell^2 + 2r_s^2(1 - \cos(\phi_1 - \phi_2)) - 2\ell r_s(\cos\phi_1 - \cos\phi_2)}$$

The centers of the fidget spinners are fixed to a base so that each spinner can only engage in rotational motion. The net torque vector (denoted by $\overrightarrow{\tau_1}$ and $\overrightarrow{\tau_2}$) creating this rotational motion for each spinner can be obtained by taking the cross product of the position vector and the force vector as shown in Equation 4.

Equation 4:

$$\begin{aligned}\overrightarrow{\tau_1}(\phi_1, \phi_2) &= \overrightarrow{r_1} \times \overrightarrow{f_1} = \frac{f_m}{\|\vec{D}\|}\, r_s(r_s \sin(\phi_2 - \phi_1) - \ell \sin\phi_1)\hat{k}, \\ \overrightarrow{\tau_2}(\phi_1, \phi_2) &= \overrightarrow{r_2} \times \overrightarrow{f_2} = \frac{f_m}{\|\vec{D}\|}\, r_s(\ell \sin\phi_2 - r_s \sin(\phi_2 - \phi_1))\hat{k}\end{aligned}$$

Since the torque is always applied along the z-axis, we will only need the magnitudes of these torque vectors, denoted by τ_1 and τ_2. Once we obtain equations for torque, we can then apply Newton's Laws of motion as shown in Equation 5, where the first term is angular acceleration and the second is viscous damping of the spinner bearing:

Equation 5:

$$\begin{aligned}J_1\, \ddot{\phi}_1 + b_1 \dot{\phi}_1 &= \tau_1(\phi_1, \phi_2), \\ J_2\, \ddot{\phi}_2 + b_2 \dot{\phi}_2 &= \tau_2(\phi_1, \phi_2)\end{aligned}$$

For the same size spinners, it is reasonable to assume that $J_1 = J_2$ and $b_1 \cong b_2$. τ_1 and τ_2 are functions of positions ϕ_1 and ϕ_2 as well as the magnetic force f_m. The magnetic force f_m will also be a complicated nonlinear function of ϕ_1 and ϕ_2. The exact form of f_m will be derived in the next section using electromagnetic theories.

Electromagnetics

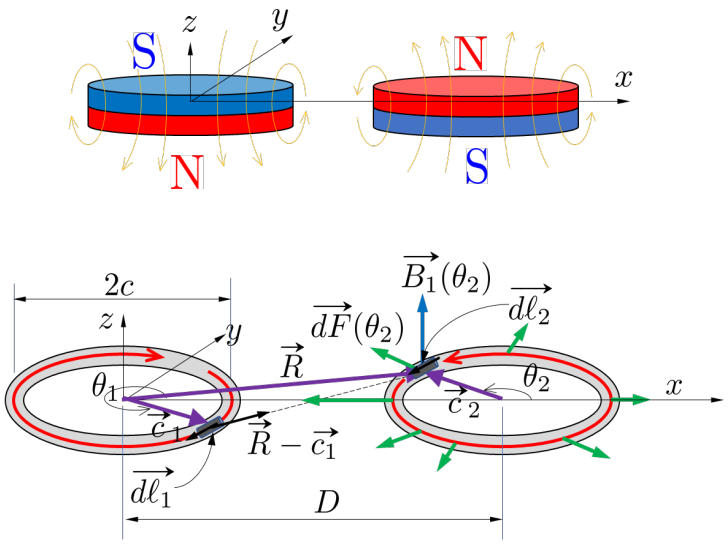

Figure 4. Configuration for electromagnetic analysis. (Upper figure) Magnetic field shape between two magnets from fidget spinners. (Lower figure) Each magnet in the upper figure can be modeled as the same size coil with its current I (the red arrow going around the ring). The small magnetic force (i.e. $\overrightarrow{dF}(\theta_2)$) experienced by the small segment of the right coil (i.e. $\overrightarrow{d\ell_2}$) can be computed by the Lorentz force equation using the magnetic field density $\overrightarrow{B_1}(\theta_2)$. On the other hand, the magnetic field density $\overrightarrow{B_1}(\theta_2)$ can be computed by the Biot-Savart law by integrating the magnetic field created by a small segment of the left coil (i.e. $\overrightarrow{d\ell_1}$). $\vec{R}$ is the position vector from the left magnet to $\overrightarrow{d\ell_2}$. c is the radius of each magnet (or the equivalent coil ring) and D is the distance between centers of two magnets.

Now, we must find component f_m in Equation 4 using the magnetic part of the theory, whose configuration is shown in Figure 4. There are two main principles we use to calculate the magnetic force: Biot-Savart law and the Lorentz force equation. We model the Nd magnet as an equivalent coil with constant current I. From (Ravaud et al., 2010), we used the following relation to find the equivalent current:

Equation 6:

$$I = \frac{m}{\pi c^2} = \frac{B_s \cdot \frac{V}{\mu_0}}{\pi c^2} = \frac{B_s h}{\mu_0}$$

where m denotes the magnetic dipole moment in $\mathrm{A \cdot m^2}$, B_s is the surface magnetic field in Tesla, $V = \pi c^2 h$ is the volume of the magnet (with h being the height or thickness of the magnet), and μ_0 is the vacuum permeability which is $1.256637 \times 10^{-6}\ \mathrm{N \cdot A^{-2}}$.

Representing the Nd magnet as a coil enables us to apply Biot-Savart law to obtain an equation for magnetic field at a point away from the loop on its plane. This point is shown by the small segment $\overrightarrow{d\ell_2}$ in Figure 4. The small segment $\overrightarrow{d\ell_2}$ experiences the magnetic field $\overrightarrow{B_1}(\theta_2)$ created by the left ring. $\vec{R}$ is the position vector from the left magnet to $\overrightarrow{d\ell_2}$. Like Equation 2, we can express these vectors using coordinate unit vectors $\hat{\imath}$ and $\hat{\jmath}$:

Equation 7:

$$\vec{R} = (D + c\cos\theta_2)\hat{\imath} + c\sin\theta_2\,\hat{\jmath},$$
$$\overrightarrow{c_1} = c\cos\theta_1\,\hat{\imath} + c\sin\theta_2\,\hat{\jmath},$$
$$\overrightarrow{c_2} = c\cos\theta_1\,\hat{\imath} + c\sin\theta_2\,\hat{\jmath},$$

$$\vec{R} - \overrightarrow{c_1} = \big(D + c(\cos\theta_2 - \cos\theta_1)\big)\hat{\imath} + c(\sin\theta_2 - \sin\theta_1)\hat{\jmath},$$
$$\overrightarrow{d\ell_1} = cd\theta_1(\sin\theta_1\,\hat{\imath} - \cos\theta_1\,\hat{\jmath}),$$
$$\overrightarrow{d\ell_2} = cd\theta_2(-\sin\theta_2\,\hat{\imath} + \cos\theta_2\,\hat{\jmath})$$

Now, the magnetic field $\overrightarrow{B_1}(\theta_2)$ is computed by integrating small segments $\overrightarrow{d\ell_1}$ of the first coil around its circumference using Biot-Savart law as Equation 8:

Equation 8:

$$\overrightarrow{B_1}(\theta_2) = \frac{\mu_0}{4\pi}\int \frac{I\overrightarrow{d\ell_1} \times \left(\vec{R} - \overrightarrow{c_1}\right)}{\left\|\vec{R} - \overrightarrow{c_1}\right\|^3} = \frac{\mu_0 I}{4\pi}\int_0^{2\pi} \frac{c - c\cos(\theta_2 - \theta_1) + D\cos\theta_1}{(2c^2(1 - \cos(\theta_1 - \theta_2)) + 2cD(\cos\theta_2 - \cos\theta_1) + D^2)^{3/2}}\, d\theta_1 \hat{k}$$

$\overrightarrow{B_1}$ is a function of θ_2 since the integration is operated for θ_1 and its direction is along the z-axis as shown by the unit vector $\hat{k}$. When this magnetic field $\overrightarrow{B_1}$ is acting on the second coil which models the second magnet, a Lorentz force is generated normal to it. Specifically, the magnetic flux $\overrightarrow{B_1}$ will create $\overrightarrow{dF}$ (colored in green in Figure 4) at the segment $\overrightarrow{d\ell_2}$. Following the Lorentz force equation, these small forces $\overrightarrow{dF}$ can be computed by the cross product of $I\overrightarrow{d\ell_2}$ and $\overrightarrow{B_1}(\theta_2)$ as shown in Equation 9:

Equation 9:

$$\overrightarrow{dF}(\theta_2) = I\overrightarrow{d\ell_2} \times \overrightarrow{B_1}(\theta_2)$$

Because $\overrightarrow{dF}$ is perpendicular to $\overrightarrow{B_1}$, $\overrightarrow{dF}$ is pointing outward and lies on the $x - y$ plane as shown by the green arrows in Figure 4. Then, the total magnetic force can be computed in turn by integrating $\overrightarrow{dF}$ over circumference of the second coil with respect to θ_2 as shown in Equation 10:

Equation 10:

$$\vec{F} = \int \overrightarrow{dF} = \int I\overrightarrow{d\ell_2} \times \overrightarrow{B_1}(\theta_2)$$
$$= \int_0^{2\pi} Icd\theta_2\,(-\sin\theta_2\,\hat{\imath} + \cos\theta_2\,\hat{\jmath}) \times \frac{\mu_0 I}{4\pi}\int_0^{2\pi} \frac{c - c\cos(\theta_2 - \theta_1) + D\cos\theta_1}{(2c^2(1 - \cos(\theta_1 - \theta_2)) + 2cD(\cos\theta_2 - \cos\theta_1) + D^2)^{3/2}}\, d\theta_1 \hat{k}$$
$$= \frac{\mu_0 I^2 c^2}{4\pi}\int_0^{2\pi}\int_0^{2\pi} \frac{\cos\theta_2\,(c - c\cos(\theta_2 - \theta_1) + D\cos\theta_1)}{(2c^2(1 - \cos(\theta_1 - \theta_2)) + 2cD(\cos\theta_2 - \cos\theta_1) + D^2)^{3/2}}\, d\theta_2 d\theta_1 \hat{\imath}$$

Because the coil is circular or symmetric with respect to its center, the y-directional components of $\overrightarrow{dF}$ will all be canceled leaving only the x-directional component (which will point left) in $\vec{F}$ as shown by the unit vector $\hat{\imath}$ at the end of Equation 10. This force $\vec{F}$ is the magnetic force experienced by the right magnet, i.e. $\overrightarrow{f_2}$ in Equation 1, and its magnitude is the magnetic force f_m of Equation 1 (or Equation 4). After integrating with respect to θ_1 and θ_2, the magnetic force f_m will be a function only of the distance D, i.e. $f_m(D)$.

Equation 11:

$$f_m(D) = \frac{\mu_0 I^2 c^2}{4\pi}\int_0^{2\pi}\int_0^{2\pi} \frac{\cos\theta_2\,(c - c\cos(\theta_2 - \theta_1) + D\cos\theta_1)}{(2c^2(1 - \cos(\theta_1 - \theta_2)) + 2cD(\cos\theta_2 - \cos\theta_1) + D^2)^{3/2}}\, d\theta_2 d\theta_1$$

Let us summarize how we computed the magnetic force $f_m(D)$. To begin with, we modeled the left Nd magnet as an equivalent coil with current I (Figure 4). Then, we computed the magnetic field $\overrightarrow{B_1}(\theta_2)$ on the right coil using Biot-Savart law (Equation 8). Once we obtained the magnetic field $\overrightarrow{B_1}(\theta_2)$ on the right coil in

terms of θ_2, we then computed the Lorentz force $\overrightarrow{dF}$ on the small segment of the right coil (Equation 8). We then found the total Lorentz force by summing up all the small Lorentz force on small segments of the right coil through another integration with respect to θ_2 (Equation 10). Due to symmetry in $\overrightarrow{dF}$ with respect to the x-axis, the net magnetic force $\vec{F}$ along the y-axis cancelled during the integration leaving the x-axis components and producing the overall net magnetic force to the left. In other words, using the Lorentz force equation and plugging it in the expression for magnetic field in Equation 8 yielded a double integral of Equation 11, which when evaluated, became a function solely of the distance D between both magnets.

As far as we know, the magnetic force $f_m(D)$ in Equation 11 does not have an indefinite integral, so it is difficult to solve analytically. Therefore, we will be discussing how to solve it numerically in the next section.

Results

To evaluate the theoretical analysis given above, we conducted simulation and experimental validation.

Simulation Results

Because the movement of the spinners is quite complicated involving double integration, we used a simulation to study it. The parameters used in the simulation are shown in Table 1. The rotational inertia is computed by adding the rotational inertia of the spinner and that of the three magnets attached at the ends of the spinner. The rotational inertia of the spinner is approximated by assuming its mass is distributed evenly over a cylinder of diameter 25 mm.

Table 1. Parameters used for the simulation.

Parameters	Notation	Values	Units
Radius of magnet	c	10	mm
Height (thickness) of magnet	h	3	mm
Surface field of magnet	B_s	1940 [i)]	Gauss
Distance between centers of spinners	ℓ	84	mm
Position of magnet from the center of spinner	r_s	28	mm
Rotational inertia of spinner and magnet (with and without metal weight at each end of spinner, these weights had been installed in the original spinner)	J_1, J_2	4.7188×10^{-5} (w/ weights) and 2.3438×10^{-5} (w/o weights)	$\text{Kg} \cdot \text{m}^2$
Equivalent current for the magnet	I	463.14 [ii)]	A

[i)] The magnetic properties from the magnet shop. https://www.kjmagnetics.com/proddetail.asp?prod=DD2

[ii)] The current is computed using Equation 6.

The code for simulation consists of the main "simulation" file and two other function files mapped in Figure 5. The main simulation has a command to solve differential equation which calls the differential equation (i.e. Equation 5) for the spinner rotary motion. The spinner rotary function module calls the double integration function (i.e. Equation 11) to obtain the magnetic force through numerical integration. Using Matlab code and built-in Runge-Kutta solver, we were able to simulate the movement of the two fidget spinners. The initial angles have been set as $\phi_1 \cong 0$ and ϕ_2 to be a little less than $2\pi/3$. (See the right figure of Figure 4 for the configuration of ϕ_1 and ϕ_2).

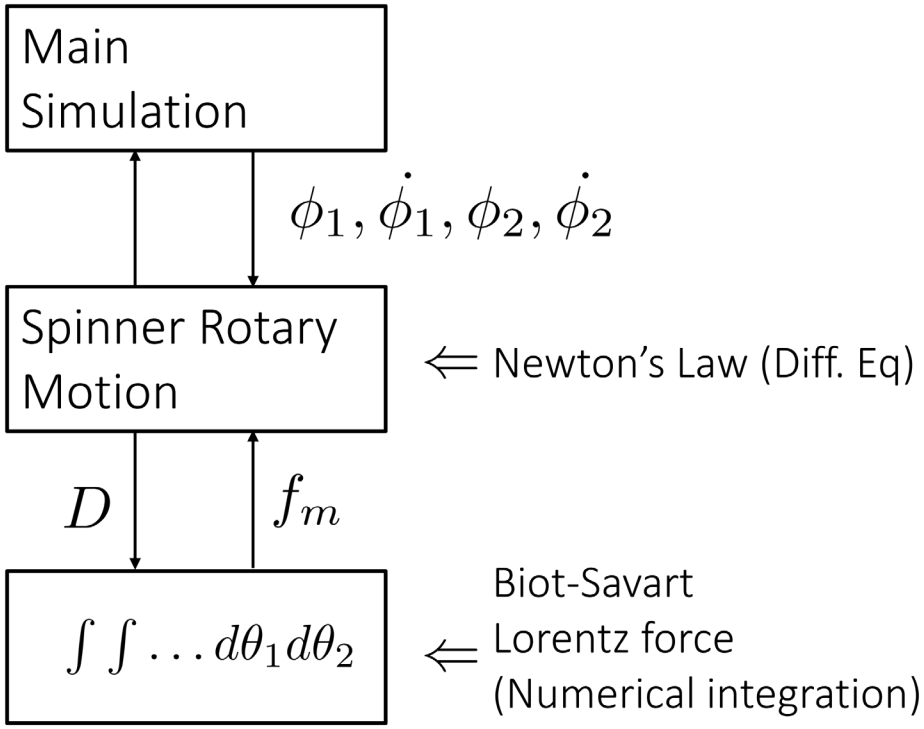

Figure 5. Simulation concept diagram.

The simulation study has been conducted by varying the viscous damping b as well as the rotational inertia J. Figure 6 shows a graph displaying rotation angle versus time produced by the simulation for a spinner with the viscous damping coefficient $b = 3 \times 10^{-5}$ Nm/(rad/s) and the rotational inertia $J = 4.7188 \times 10^{-5}$ kg·m^2. This value of J represents the rotational inertia of the spinner in its original form. This value of b was chosen such that it yielded reasonable dissipation (decay) rate of the nonlinear oscillation. The initial positions of the spinners have been set as $\phi_1(t = 0) = 0.075$ rad and $\phi_2(t = 0) = 1.04 \times 2\pi/3$. These values were obtained from the initial values of the experimental results which will be presented in the next section.

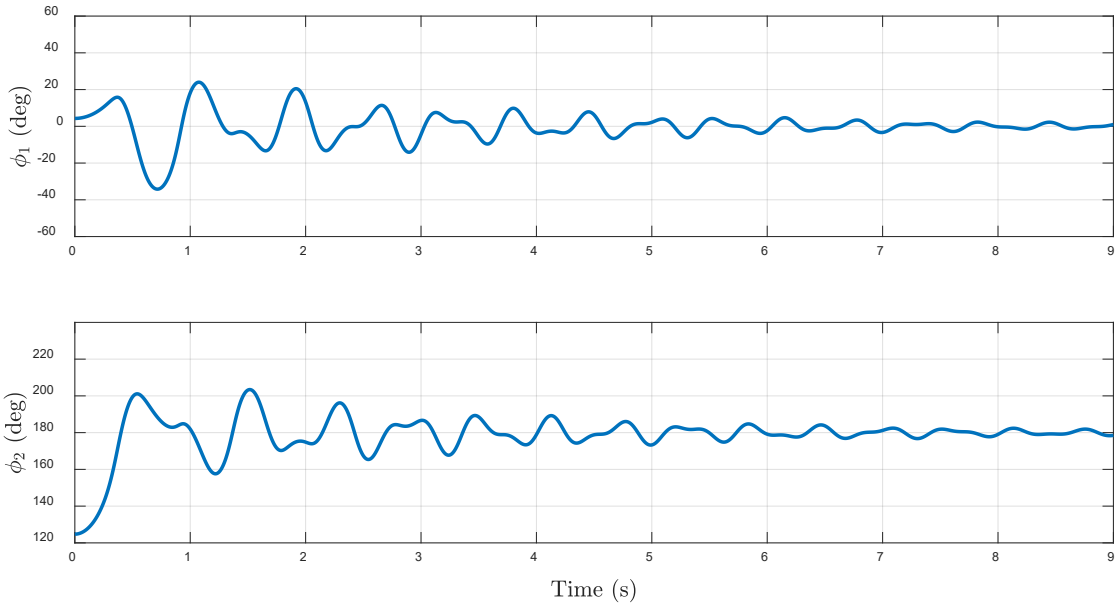

Figure 6. Simulation result of oscillation of magnetic gear spinners with $b = 3 \times 10^{-5}$ Nm/(rad/s) and $J = 4.7188 \times 10^{-5}$ kg·m^2.

Figure 7 shows another simulation with the smaller viscous damping coefficient $b = 5 \times 10^{-6}$ Nm/(rad/s) and the smaller rotational inertia $J = 2.3438 \times 10^{-5}$ kg·m^2 which represents the case where we removed the metal weights on the ends of spinners. Compared to Figure 6, Figure 7 shows oscillations with higher frequency and less dissipation, i.e. the oscillation persists longer.

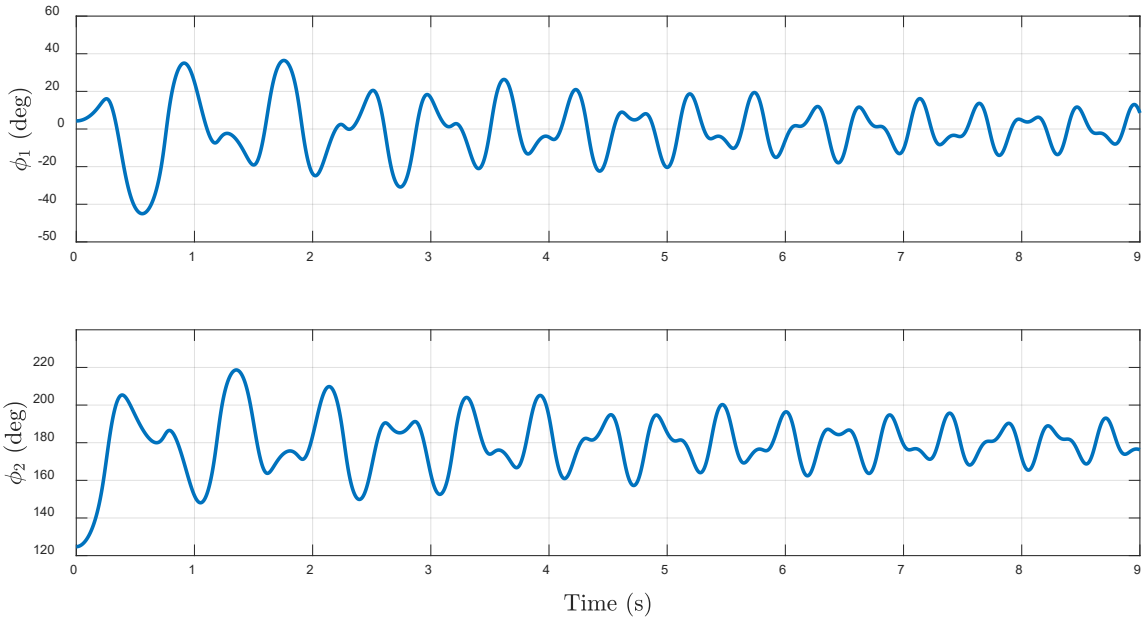

Figure 7. Simulation result of oscillation of magnetic gear spinners with $b = 5 \times 10^{-6}$ Nm/(rad/s) and $J = 2.3438 \times 10^{-5}$ kg·m^2.

Experimental Validation

We conducted experiment using the spinners arranged as shown in Figure 1. The parameters given in Table 1 represent actual parameters for the experimental setup. For the rotational inertia, we removed the metal weights from the spinners, so the value used in the experiment was $J = 2.3438 \times 10^{-5}$ kg·m^2. The experiment was performed by taking videos of the movement of spinners. We used the iPad Pro to take videos with slow motion setting allowing us to take videos at a relatively high frame rate (i.e. 240 frames per second). Figure 8 shows the configuration of the iPad and spinners for recording. As shown in the figure, small circular markers with different colors are attached to the magnets and centers of spinners so that we can track them from an image processing software. We used the program called the Physics Tracker[1] which is widely used for analyzing videos taken for various physics experiments. Figure 9 shows the screenshot of Tracker generating data from the recorded video.

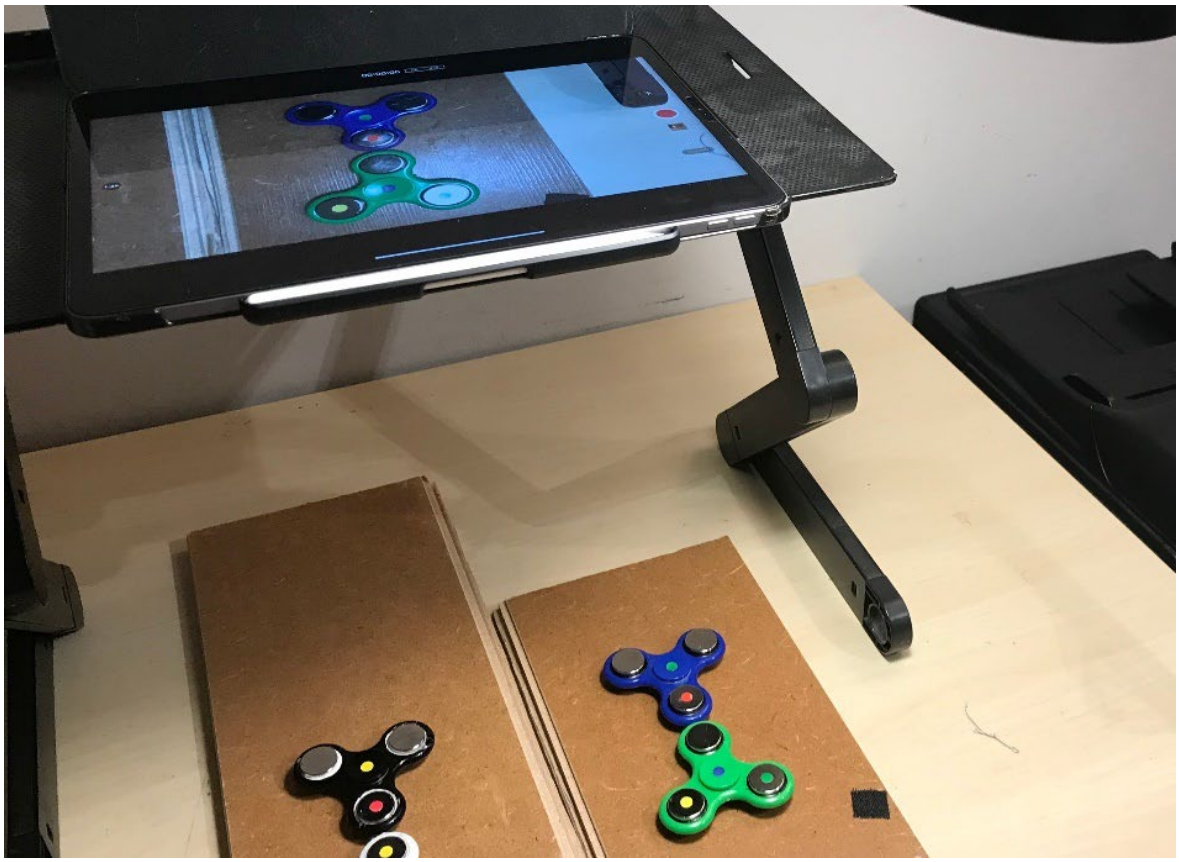

Figure 8. Top view of experimental setup.

After a few trials with different values of the damping coefficient, we obtained the corresponding simulation results with $b = 1.2 \times 10^{-5}$ Nm/(rad/s) and other parameters same as Table 1. Simulation and experimental plots are shown in Figure 10 for comparison.

[1] https://physlets.org/tracker/

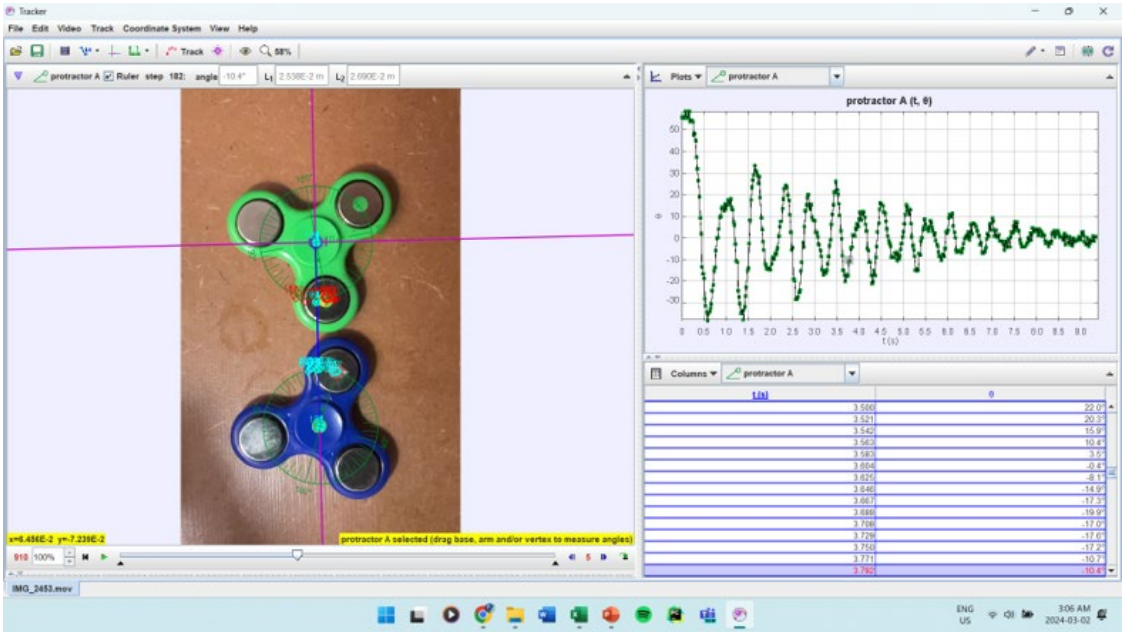

Figure 9. Screenshot of how Tracker is used to obtain rotational angles of spinners.

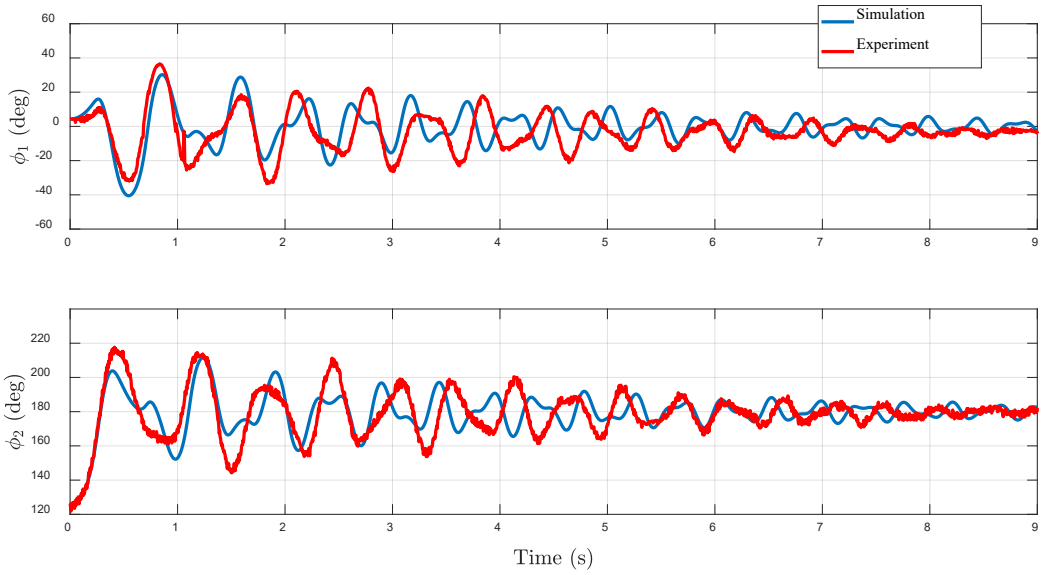

Figure 10. Experimental results and their comparison with simulation results.

Discussion

In a typical mass-spring damper system where the oscillation is linear, we see single frequency sinusoid with exponential decay. However, as we can see in Figures 6 and 7, the oscillation of the fidget spinners is far from a linear oscillation with signals largely distorted. Also, the decay rate (dissipation) is not exponential. These are due to the nonlinear magnetic force which we derived in Equation 11. Figure 10 shows that our analytic results well describe the actual behaviour of the nonlinear oscillation.

In contrast to linear oscillation, as we can see in Figures 6 and 7, the oscillation is far from a perfect single-frequency sinusoid due to nonlinear effects of the magnetic force. As a result, the plot is largely distorted. The decay rate is also far from the exponential shape that we observe in linear vibration. Meanwhile, we can also observe that the results in Figures 6 and 7 reveal some qualitative behaviors that have the same tendency as those observed in linear systems; 1) the more the inertia, the slower the overall frequency and 2) the bigger the viscous damping, the more the dissipation (or decay).

According to Figure 10, the first few cycles have good match, but after a while, more deviation occurs between simulation and experimental results. We can provide some postulations as to the cause of this variation. First, we approximated the permanent magnet as an equivalent coil, which is not exactly the case due to nonuniform magnetic field distribution. This point has been supported by Taniguchi (2018) who used elliptic integrals to compute the exact magnetic field of a ferromagnetic cylinder. Second, we reasonably approximated the viscous damping on the bearing of the spinner to be linear. However, the constantly changing magnetic fields experienced by either magnet moving relative to the other may cause an eddy current effect in the form of circular currents, which may not be linear. Third, there is random noise and uncertainty in the physical experiment. Deviation occurs a while after the first few cycles because the effect of noise gets accumulated. Over time, these deviations become more pronounced due to unmodeled effects.

In the future, it would be useful to investigate unaccounted factors such as nonuniform magnetic field and eddy currents to obtain more realistic simulation results. We would also like to design a more accurate model by investigating cases in which deflection is greater than the aforementioned angle or giving the spinner a constant applied force. Varying more key parameters such as number of arms would also provide more complete research of the phenomenon.

Conclusion

Our investigation of the underlying mechanics of the magnetic gear phenomenon yielded several new findings. The exact mathematical form of the magnetic force between two neodymium magnets in this specific configuration was not available in literature, so we resorted to fundamental theories to derive it. In the limiting case where the spinner is pulled at an initial deflection of 3π radians, energy transfer between both spinners is apparent. Although the initial theoretical model presented is much simpler in nature, it was consistent with the integration of mechanics through rotational inertia and magnetics through the application of Biot-Savart law and the Lorentz force equation. Moreover, our theoretical analysis made use of a simulation to quantitatively control key variables. Specifically, we were able to exactly model and experimentally validate the dissipation of rotation angle over time attributed to viscous damping. Finally, we investigated the effects of varying relevant parameters, namely rotational inertia and viscous damping through simulation and experiment.

Acknowledgments

I would like to thank my school for lending me the PASCO magnetic field sensor, as well as my peers who encouraged me throughout the process.

References

Purcell, E. M., & Morin, D. J. (2013). *Electricity and magnetism*. Cambridge university press.

Ravaud, R., Lemarquand, G., Babic, S., Lemarquand, V., & Akyel, C. (2010). Cylindrical magnets and coils: Fields, forces, and inductances. IEEE Transactions on Magnetics, 46(9), 3585-3590. https://doi.org/10.1109/TMAG.2010.2049026

Taniguchi, T. (2018). An analytical computation of magnetic field generated from a cylinder ferromagnet. *Journal of Magnetism and Magnetic Materials*, *452*, 464-472.

Tlali, P. M., Wang, R. J., & Gerber, S. (2014, September). Magnetic gear technologies: A review. In 2014 International Conference on Electrical Machines (ICEM) (pp. 544-550). IEEE. https://doi.org/10.1109/ICELMACH.2014.6960233

Vila, J., Paulino, G. H., & Ruzzene, M. (2019). Role of nonlinearities in topological protection: Testing magnetically coupled fidget spinners. Physical Review B, 99(12), 125116. https://doi.org/10.1103/PhysRevB.99.125116

Vokoun, D., Beleggia, M., Heller, L., & Šittner, P. (2009). Magnetostatic interactions and forces between cylindrical permanent magnets. Journal of magnetism and Magnetic Materials, 321(22), 3758-3763. https://doi.org/10.1016/j.jmmm.2009.07.030